THE JOURNAL OF PHYSICAL CHEMISTRY B

Article

pubs.acs.org/JPCB

Free-Volume Theory Coupled with Soft-SAFT for Viscosity Calculations: Comparison with Molecular Simulation and Experimental Data

F. Llovell,*[,†] R. M. Marcos,[‡] and L. F. Vega[†,§]

[†]MATGAS Research Center, Campus de la UAB, 08193 Bellaterra, Barcelona, Spain

[‡]Departament d'Enginyeria Mecànica, ETSE, Universitat Rovira i Virgili, 43007 Tarragona, Spain

[§]Carburos Metálicos/Air Products Group, C/Aragón, 300, 08009 Barcelona, Spain

Supporting Information

ABSTRACT: The evaluation of phase equilibria and solubility properties through theoretical approaches is a well-known field, where a significant amount of models are able to describe them with a good degree of accuracy. However, the simultaneous calculation of transport properties together with thermodynamic phase properties still remains a challenge, due to the difficulties in describing the behavior of properties like the viscosity of fluids with the same approach. In this work, the free-volume theory (FVT) has been coupled with the soft-SAFT equation for the first time to extend the capabilities of the equation to the calculation of transport properties. The theory has been first tested using simulation data of the viscosity of the Lennard-Jones (LJ) fluid and LJ chains over a wide range of temperature and pressure. Good agreement has been found at all chain lengths, except for some deviations at near-zero density values. Several trends of the viscosity parameters with the length of the chain are identified, allowing the prediction of other chain fluids. Finally, the new equation has been applied to the *n*-alkanes family, where viscosity is a key property, and results are compared with experimental data. The three viscosity parameters were fitted to viscosity data of the pure fluid at several isotherms or isobars, whereas the density and pressure (or temperature) were taken from the soft-SAFT output. Again, the effect of these parameters on the viscosity has been investigated and compared with results obtained for the LJ chains and with previous work of other authors. The new equation performs very well in all cases, with a global average absolute deviation of 2.12% and shows predictive capabilities for heavier compounds. This empowers soft-SAFT with new capabilities, allowing the equation to calculate phase, interfacial, and transport properties with the same model and degree of accuracy.

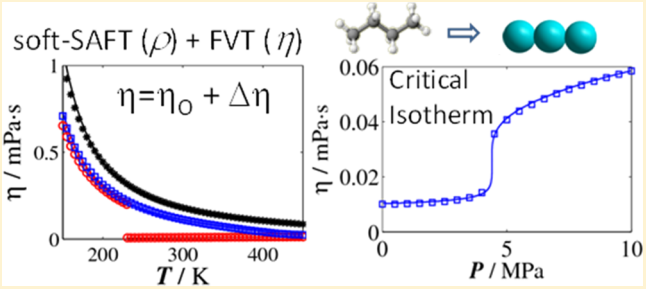

1. INTRODUCTION

An accurate description of transport properties and, in particular, of dynamic viscosity is necessary for the design of surface facilities in a wide variety of industrial processes. Liquid viscosity has a direct and large effect on heat transfer coefficients, which are especially important for heat exchangers and various heat transfer considerations, as well as in distillation calculations. Viscosity data are also essential for calculating pressure drops, as for pump and piping calculations, becoming a critical property in the chemistry and petroleum industry, and in many types of manufacturing practices. The viscosity of a substance determines how it should be handled, stored, and discarded. As a consequence, this property has been extensively investigated from an experimental point of view for a wide variety of fluids.

From a modeling perspective, many approaches for describing the viscosity of fluids are available in the literature, going from entirely empirical to highly theoretical. The reader is referred to critical reviews on this topic.[1−3] On one hand, empirical methods, mainly based on correlations, are easy to compute and provide good results, but they lack extrapolation capability and can only be applied to a particular range of conditions. On the other hand, theoretical methods, like the Chapman−Enskog theory, are accurate for the calculation of dilute-gas viscosities, but they fail when reproducing the viscosity of a dense fluid. In the last decades, several new models, based on theoretical approaches, have been proposed for the calculation of dense fluids and have achieved a certain degree of success. Among them, the most popular are the hard-sphere scheme,[4,5] the free-volume theory (FVT),[6,7] the friction theory (FT) and further developments,[8−10] extensions of the kinetic-theory to chains,[11,12] scaling relations with the residual (or excess) entropy,[13−15] or equations obtained from fitting to molecular-dynamic simulation results.[16−19] All of them have advantages and disadvantages, and still none of them is able to estimate the viscosity of fluids in a fully predictive manner.

Received: February 5, 2013
Revised: June 20, 2013
Published: June 21, 2013

dx.doi.org/10.1021/jp401307t | J. Phys. Chem. B 2013, 117, 8159−8171

Hence, there is still room to explore the possibilities of these methods and to develop new ideas.

In the particular case of the FVT, there are several contributions where the treatment has been applied to the calculation of pure fluids. In the original article of Allal and co-workers,[6] where the theory is presented, FVT was tested for 41 compounds of very different chemical families: alkanes (linear and ramified, light and heavy), alkylbenzenes, cycloalkanes, alcohols, fluoroalkanes (refrigerants), carbon dioxide, and water, with excellent agreement in all cases. In the same year, the authors extended the theory to the vapor phase and tested it with *n*-alkanes, *trans*-decalin, benzene, and 2,2-dimethylpropane.[7] Finally, they also included the calculation of self-diffusion coefficients,[20] and a simultaneous calculation of both properties (viscosity and self-diffusion coefficient) using the same parameters was provided for some compounds, including benzene, carbon tetrachloride, chlorotrifluoromethane, cyclohexane, methylcyclohexane, and tetramethylsilane. Baylaucq et al.[21] modeled the density and the viscosity of four pure substances (dimethylcarbonate, diethyl carbonate, triethylene glycol dimethyl ether and tetraethylene glycol dimethyl ether) with different methodologies, including FVT. They reached very good agreement with the experimental data (absolute average deviation (AAD) ranging from 0.9% to 2.3%). In another study from the same research group,[22] they studied the effect of stereoisomerism on dynamic viscosity, modeling the *cis*-decalin and *trans*-decalin compounds with FVT. They obtained very good agreement with the experimental measurements from their laboratory (less than 1% of AAD) and showed that the characteristic molecular length and the molecular overlap of FVT are strongly related to the structural configuration of the stereoisomeric decalin molecules. In a collaborative work between the University of Pau (France) and the University of Santiago de Compostela (Spain), two contributions focused on the influence of the molecular structure of alkoxyethanols on the viscosity of those compounds using FVT were published.[23,24] The authors accurately reproduced the experimental viscosity (around 2% of AAD) and were able to correlate the parameters of the theory against the number of CH_2-CH_2-O groups.

In almost all the contributions mentioned in the previous paragraph, the density, which is an input required for the calculation of viscosity with FVT, was either experimentally determined or taken from correlated data. In fact, the simultaneous evaluation of thermodynamic and transport properties of fluids using semitheoretical viscosity approaches, such as FT or FVT, in conjunction with sophisticated equations of state (EoSs) is not abundant, even if in many viscosity approaches a precise calculation of the viscosity requires an accurate prediction of other properties of the system, such as the density and/or the pressure. In this regard, statistical associating fluid theory type (SAFT-type) EoSs can become an excellent platform so as to provide these properties with a high degree of accuracy. Unfortunately, and in spite of the attractiveness of the approach, there are not too many contributions available in the literature pointing in that direction. Tan et al.[25] used FVT and FT to estimate the viscosity of pure *n*-alkanes using the SAFT1 and PC-SAFT EoSs. Later on, they extended the work to mixtures of *n*-alkanes using only FT.[26] Quiñones-Cisneros and collaborators had also developed a generalized friction theory (GFT) model for the PC-SAFT EoS and have applied it to *n*-alkanes and to mixtures between *n*-alkanes and with carbon dioxide.[10,27] Goel et al.[13] and Galliero et al.[14] used a scaling approach of the viscosity with the excess entropy, obtained from the SAFT and LJ-SAFT EoSs, respectively, to calculate the viscosity of Lennard-Jones chains simulations, as well as argon and some normal alkanes in the case of the work of Galliero and collaborators. In another scaled approach, Novak used the residual entropy and the segment parameter from the PC-SAFT EoS to describe the viscosity of *n*-alkanes and some polymers.[15] Polishuk used the recently proposed SAFT + Cubic EoS coupled with the modified Yarranton-Satyro correlation to model the viscosity in an extended pressure range of a variety of hydrocarbons, gases and ionic liquids.[28] Moreover, he compared the performance of the correlation with the friction theory + PC-SAFT of Quiñones-Cisneros et al.[27] and the work of Novak previously mentioned.[15] Finally, in a very recent contribution, Burgess et al. have used both FVT and FT approaches in combination with PC-SAFT for the calculation of the viscosity of *n*-alkanes up to C_{18}, branched alkanes, single and double ring aromatics and naphtalenic compounds up to extreme pressure conditions (276 MPa) for applications in ultradeep porous sandstone or carbonate layers that retain crude oil or natural gas.[29]

The work presented here uses FVT coupled with the crossover soft-SAFT EoS to describe the viscosity of fluids with a high degree of accuracy and in a way as predictive as possible. The crossover soft-SAFT EoS[30−32] is used as a basis for the evaluation of the necessary thermodynamic properties. The choice of soft-SAFT is based on its accuracy to describe the phase diagrams (and the density in particular) of a wide variety of families and mixtures, such as *n*-alkanes,[31−38] *n*-perfluoroalkanes,[39−41] hydrofluorocarbons,[42] 1-alkanols,[32] and ionic liquids,[43−46] in broad ranges of temperature and pressure. This is a step forward into extending the capabilities of a molecular-based EoS, such as soft-SAFT, for engineering purposes. The addition of FVT allows calculations of thermophysical and transport properties with the same equation and molecular model.

The rest of the paper is organized as follows: the next section includes a complete presentation of FVT, as well as a brief description of the soft-SAFT EoS, being linked by the calculation of both the density and the pressure (or, temperature, depending if an isotherm or an isobar is calculated). Then, the accuracy of the extended equation is checked versus molecular simulations of the Lennard-Jones fluid and Lennard-Jones chains of different length. The influence of the viscosity parameters and the trends observed with the number of monomers are studied in more detail. Next, the theory is applied to the most common family of hydrocarbons, where knowledge of the viscosity plays a key role: the *n*-alkanes. Some concluding remarks are provided at the end.

2. THEORY

2.1. FVT. The FVT model used in this work was developed by Allal et al. in 2001,[6,7] based on both the previous free-volume concepts and diffusion models applied to viscosity and originally proposed in earlier contributions by other authors.[47,48] The original work of Allal and co-workers was only valid for dense fluids,[6] while a new version extending the capabilities of the equation to low-density states was published in the same year.[7] The work presented here is based in this latter approach. In the following equations, viscosity is given in mPa s.

dx.doi.org/10.1021/jp401307t | J. Phys. Chem. B 2013, 117, 8159−8171

FVT connects the viscosity to the molecular structure of the fluid, and is formulated to correctly describe the low-dense to dense state transition. This approach divides the contribution to the viscosity in two terms: the diluted gas term and the dense liquid term

$$\eta = \eta_0 + \Delta\eta \tag{1}$$

where η_0 is the viscosity of the dilute gas and $\Delta\eta$ is the dense-state correction term. The idea of this separation was originally proposed by Quiñones-Cisneros et al.[8] for the friction theory, in order to separate the purely kinematic physics of the dilute gas limit from the more complex physics that involves the dense state, and was later used by Allal et al. for FVT.[7] The correction term vanishes when the fluid system approaches the dilute gas limit.

The dilute gas term describes the viscosity of a fluid in the gaseous state or with a very low density. The kinetic theory of Chapman-Enskog[49] is a theoretical predictive approach that treats the interaction between colliding rigid spheres of a certain diameter and mass. However, this original model did not take into account the nonsphericity of the molecules or the presence of anisotropic molecular forces. Chung et al.[50] modified the original Chapman-Enskog theory and introduced a correction factor F_c to include the effects of chain bonding, hydrogen bonding and polarity. The modified equation is used here and reads

$$\eta_0 = 40.785 \times 10^{-2} \frac{\sqrt{M_w T}}{{v_c}^{2/3}\Omega^*(T^*)} F_c \tag{2}$$

where T is the temperature (K), M_w is the molecular weight (g/mol), v_c is the critical volume (L/mol), and Ω^* is the reduced collision integral. This integral depends on the intermolecular potential chosen and is a complex function of the temperature. Neufeld et al.[51] was able to determine the collision integral for the Lennard-Jones potential and proposed an empirical correlated expression

$$\Omega(2;2) = \frac{1.16145}{T^{*0.14874}} + \frac{0.52487}{\exp(0.77320T^*)} + \frac{2.16178}{\exp(2.43787T^*)} - 6.435 \times 10^{-4} T^{*0.14874} \sin(18.0323T^{*-0.76830} - 7.27371) \tag{3}$$

As mentioned, the expression depends on a dimensionless temperature $T^* = 1.2593T_r$, being T_r the reduced temperature respect to the critical temperature of the compound (K). F_c is the empirical factor introduced by Chung et al.[50]

$$F_c = 1 - 0.2756\omega - 0.059035{\mu_r}^4 - \kappa \tag{4}$$

The correction includes the acentric factor ω of the compound to account for the nonsphericity of the compound, the dipole moment μ of the molecule (Debye) to consider polar effects, and an empirical parameter κ to account for hydrogen bonding formation. All of the molecules of this work are considered with $\mu = 0$ and $\kappa = 0$, because n-alkanes have either a very low or zero dipole moment and do not have hydrogen bonding. Hence, eq 4 is reduced to $F_c = 1 - 0.2756\omega$

The dense-state term comes from linking two different ideas. From one side, the viscosity is believed to be connected to the microstructure of the fluid based on a generalized dumbbell model[6,7]

$$\Delta\eta = 10^{-14}\rho N_a \zeta L^2 \tag{5}$$

where ρ is the density (mol/L), N_a is the Avogadro's number (mol^{-1}), ζ is a friction coefficient related to the diffusion process and the mobility of the molecule (kg/s), and L^2 is an average quadratic length related to the size of the molecule (Å^2).

From the other side, the concept of the viscosity as dependent on the empty space between molecules allows the definition of a free-volume fraction f_v. It is then assumed that the viscosity is related to the free-volume fraction through an exponential relation, according to the behavior observed experimentally for the molecular transport of liquids and glasses[48,52]

$$\Delta\eta = A \exp\left(\frac{B}{f_v}\right) \tag{6}$$

The combination of eqs 5 and 6 allows the friction coefficient to be written as

$$\zeta = \zeta_0 \exp\left(\frac{B}{f_v}\right) \tag{7}$$

and consequently

$$\Delta\eta = 10^{-14}\rho N_a L^2 \zeta_0 \exp\left(\frac{B}{f_v}\right) \tag{8}$$

In eqs 6−8, B is a parameter related to the free-volume overlap among the molecules. The free-volume fraction is defined as the ratio between the free molecular volume available v_f and the total molecular volume v. This ratio can also be related to the potential energy of interaction E (J)

$$f_v = \left(\frac{RT}{E}\right)^{3/2} \tag{9}$$

R being the universal constant for gases (J/mol K). It is then assumed that the potential energy of interaction is a sum of two terms, an ideal gas term and a second term directly related to the density

$$E = \frac{10^3 P}{\rho} + \alpha\rho M_w \tag{10}$$

with P being the pressure of the system (MPa). The first term is related to the energy necessary to form the vacant vacuums available for the molecular diffusion. The second term is connected to the energy barrier that the molecule has to cross to diffuse, that will depend on the density and on an activation energy parameter α (J m^3/mol kg).

ζ_0 (kg/s) is coming from the friction coefficient and is related to the force of dissipation F (N) by the expression:

$$F = \zeta_0 \bar{v} \tag{11}$$

where $\bar{v}$ is the speed of dissipation (m/s). The force of dissipation is related to the energy of dissipation E given in a certain length of dissipation b_f (Å). An additional assumption is made in the treatment by considering that all the thermal energy of activation is transformed into kinetic energy. With all of these considerations, ζ_0 can be rewritten as

dx.doi.org/10.1021/jp401307t | J. Phys. Chem. B 2013, 117, 8159−8171

$$\zeta_0 = 10^{10}\frac{E}{N_a b_f}\left(\frac{10^{-3}M_w}{3RT}\right)^{1/2} \quad (12)$$

If we combine eqs 8−10 and 12, a final expression for the dense fluid term in mPa s can be given

$$\Delta\eta = L_v(0.1P + 10^{-4}\alpha\rho^2 M_w)\sqrt{\frac{10^{-3}M_w}{3RT}} \exp\left[B\left(\frac{10^3 P + \alpha\rho^2 M_w}{\rho RT}\right)^{3/2}\right] \quad (13)$$

Or in an equivalent condensed free-volume dependent expression, it reads

$$\Delta\eta = 10^{-4}\rho L_v\sqrt{\frac{10^{-3}RTM_w}{3}} f_v^{-2/3} \exp\left[\frac{B}{f_v}\right] \quad (14)$$

where L_v (Å) is L^2/b_f.

The previous equation relates the molecular structure with a representation of the free-volume fraction, and this fraction with the intermolecular energy controlling the potential field in which the molecular diffusion takes place.[7]

The final equation includes three adjustable parameters: L_v is a length parameter related to the structure of the molecules and the characteristic relaxation time, α is the proportionality between the energy barrier and the density, and B corresponds to the free-volume overlap. These parameters are fitted to available experimental viscosity data.

The description of the viscosity requires previous calculation of some thermodynamic properties, mainly the density and the pressure/temperature of the system. The accuracy of the calculated viscosity heavily relies on the accurate calculation of those properties. Hence, it is important to choose a reliable method to calculate the thermodynamic input; in this work, we use the soft-SAFT equation as it has proven to be a reliable EoS for ideal and highly nonideal systems. We have incorporated FVT treatment into the code for soft-SAFT calculations developed and optimized by our research group, so that all properties are provided within the same source.

2.2. Soft-SAFT EoS. Soft-SAFT[30,35] is an EoS belonging to the well-known SAFT family, developed from the original SAFT EoS.[53,54] Based on Wertheim's first-order thermodynamic perturbation theory (TPT1),[55−58] the equation is built up as a sum of molecular terms that contribute to the total free energy of the system and it is firmly grounded in statistical mechanics. The description of soft-SAFT has been addressed in detail in previous publications,[30,35] and only the main features are retained in the present discussion.

The general expression for the soft-SAFT equation is given in terms of the residual Helmholtz energy, a^{res}, obtained as a sum of the different microscopic contributions

$$a^{res} = a - a^{id} = a^{ref} + a^{chain} + a^{assoc} + a^{polar} \quad (15)$$

where a and a^{id} are the total and ideal Helmholtz energy density of the fluid of interest at the same temperature and density, respectively. a^{ref} is the reference contribution to the Helmholtz energy of the spheres composing the molecules; a^{chain}, the chain contribution term, and a^{assoc}, the association term, come from Wertheim's TPT1 theory;[55−58] finally, a^{polar} refers to a specific term accounting for polarity. In this work, the association and the polar term of the soft-SAFT equation are set to zero, as the fluids treated here (Lennard-Jones chains and *n*-alkanes) are considered nonpolar and nonassociating.

The reference term in the soft-SAFT EoS accounts for the dispersive and repulsive forces between the monomers using a Lennard−Jones (LJ) intermolecular potential as the reference fluid. The monomers are characterized by two molecular parameters: the segment diameter, σ_{ii}, and the dispersive energy between segments, ε_{ii}. This term is described following the EoS of Johnson et al.[59]

The chain term, a^{chain}, accounts for the energy of formation of chains from units of the reference fluid (monomers). This term is obtained by taking the limit of complete bonding in Wertheim's TPT1 theory, and it is formally identical in all versions of SAFT. The Helmholtz free energy due to the formation of chains from m_i spherical segments can be written as:

$$a^{chain} = \rho k_B T \sum_i x_i(1 - m_i)\ln g_{LJ} \quad (16)$$

where ρ is the molecular density of the fluid, T is the temperature, k_B is the Boltzmann constant, m_i the number of segments of component i, and x_i is its mole fraction. g_{LJ} is the radial distribution function of the reference fluid at contact, which is obtained from the expression of Johnson et al.[60]

The classical formulation of SAFT is based on the mean-field assumption and makes the theory unable to correctly describe the scaling of thermodynamic properties as the critical point is approached. In order to overcome this limitation, a renormalization group treatment, based on White's methodology,[61−63] is incorporated into the equation. The approach reproduces the asymptotic behavior close to the critical point, while reducing to the original EoS far from it. Mathematically, it is expressed as a set of recursive equations that incorporates the density fluctuations in a progressive way

$$a = \rho k_B T \sum_{i=1}^{\infty}(a_{i-1} + \Delta a_i^{cross}) \quad (17)$$

The value of a_{i-1} for the first iteration corresponds to the original soft-SAFT value, and Δa_i^{cross} is the contribution of each wave packet of fluctuations considered in the system, accounted as a ratio between a non mean-field and a mean-field treatment

$$\Delta a_i^{cross}(\rho) = -K_i\frac{\Omega^s(\rho)}{\Omega^l(\rho)} \quad (18)$$

where Ω^s and Ω^l represent the density fluctuations for the short-range and the long-range attractions, respectively, and K_i is a coefficient that depends on the temperature and the cutoff length. The inclusion of the crossover treatment leads to two additional parameters, the cutoff length, L, and the average gradient of the wavelet function, ϕ. These parameters are treated as adjustable when using the equation for real fluids and fitted to experimental data. The reader is referred to the original crossover soft-SAFT papers for more details about the theory and its implementation.[31,32]

The performance of soft-SAFT with and without the crossover term for the vapor−liquid equilibria of LJ chains and the *n*-alkanes family has already been presented in the literature.[30,31,35] The soft-SAFT molecular parameters and the results for the density−temperature diagram versus simulation and experimental data, respectively, are presented in the Supporting Information for completeness.

dx.doi.org/10.1021/jp401307t | J. Phys. Chem. B 2013, 117, 8159−8171

3. RESULTS AND DISCUSSION

3.1. Comparison with Molecular Simulations. The FVT has been tested using simulation data of the viscosity of the LJ fluid and LJ chains. This is a very interesting test to evaluate the implemented treatment, as the results can be compared with molecular simulations that rely under the same molecular model and there are no adjusted soft-SAFT molecular parameters that could hide the performance of the viscosity theory. For this purpose, we have used the simulation data published by Galliero, Boned and co-workers in a series of three different papers for the LJ fluid[16] and LJ chains using a fully flexible and a rigid model.[17,64] The comparison has been made using the simulation data values provided with the fully flexible model.

All the variables are reduced using the LJ molecular parameters σ and ε, and also with the molecular weight M_w or the chain length m. The viscosity parameters α^*, and L_v^* (B is already dimensionless) are reduced as follows:

$$\alpha^* = \alpha \frac{10^{-3} M_w}{\varepsilon \sigma^3 N_A} \tag{19}$$

$$L_v^* = \frac{L_v}{\sigma} \tag{20}$$

Results concerning the viscosity of the LJ fluid are presented in Figure 1. A description of the viscosity-density (Figure 1a), viscosity-pressure (Figure 1b) and viscosity-temperature (Figure 1c) diagrams, covering a range of reduced densities from $\rho^* = 0$ to 1.1 and a range of reduced temperatures from $T^* = 0.7$ to 4 is shown. The symbols represent the simulation data while the curves are the soft-SAFT + FVT calculations. The critical properties needed for the calculation of the diluted term have been taken from the literature.[59] The reduced viscosity parameters α^*, B^*, and L_v^* have been fitted to these data and are indicated in Table 1. The density and pressure values needed were directly obtained from the soft-SAFT equation by only considering the ideal and the reference term (a LJ fluid). In all cases, excellent agreement in the whole range of temperature, pressure and density is achieved with a common set of viscosity parameters.

Figure 2 depicts the description of the viscosity of LJ chains. Figure 2a–d represents the viscosity-density diagram of dimers ($m = 2$), tetramers ($m = 4$), octamers ($m = 8$), and hexadecamers ($m = 16$), respectively. The procedure followed is the same described above, with the three viscosity parameters being adjusted to the simulation data. The critical properties and the acentric factor for $m = 2$ and $m = 4$ have been taken from a reference of the same authors.[65] An approximate value of the acentric factor for octamers and hexadecamers was calculated by extrapolation of the values from shorter LJ chains from the previous reference, while the critical temperature and volume were obtained from ref 66. The ranges of density and temperature studied, along with the optimized viscosity parameters, are included in Table 1. Once more, very good agreement is achieved in all cases, although an increase in the absolute average deviation (AAD%) and the maximum deviation (MxD%) when increasing the chain length is observed (see Table 1). This is due to some deviations when approaching the zero-density viscosity, which depends mostly on the diluted term of FVT, leading to higher errors at low density. Galliero and co-workers had also reported the issue in their previous work[17] and suggested to modify the Chapman-Enskog theory by including a chain length dependence, as follows:

$$\eta_0^* = \frac{5}{16\Omega^*(T^*)} \sqrt{\frac{T^*}{m\pi}} \tag{21}$$

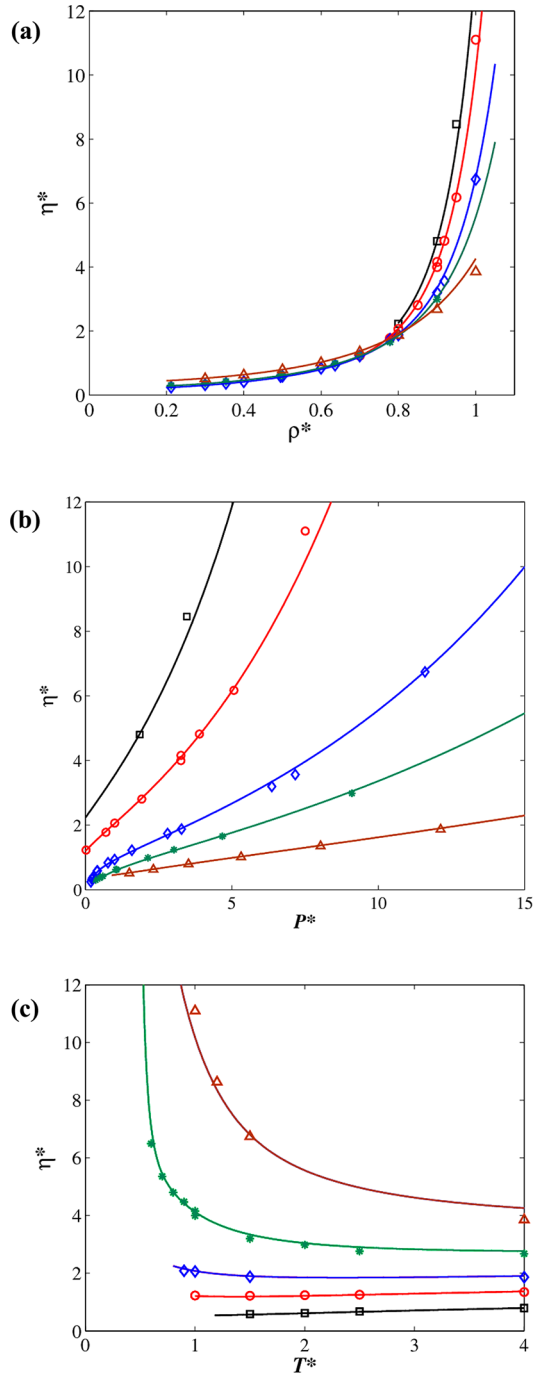

Figure 1. Reduced viscosity of the Lennard-Jones fluid. (a) Viscosity–density diagram at five isotherms $T^* = 0.8$ (black square), 1.0 (red circle), 1.5 (blue diamond), 2.0 (green asterisk), and 4.0 (brown triangle) (b) Viscosity-pressure diagram at the same five isotherms (c) Viscosity-temperature diagram as a function of temperature at five isopleths $\rho^* = 0.5$ (black square), 0.7 (red circle), 0.8 (blue diamond), 0.9 (green asterisk), and 1.0 (brown triangle). In all panels, symbols represent the experimental data,[16] while the curves correspond to the soft-SAFT + FVT modeling.

dx.doi.org/10.1021/jp401307t | J. Phys. Chem. B 2013, 117, 8159–8171

Table 1. Optimized Characteristic Parameters of FVT for Simulations of Lennard-Jones Chains[a]

N_c	N_{points}	ρ_{mon}*	T*	α*	B*	L_v*	AAD (%)	MxD (%)
1	92	0.1−1.0	0.7−4	12.44	0.01610	0.2061	2.78	10.8
2	62	0.1−1.1	0.7−6	50.47	0.00723	0.2246	4.71	22.3
4	54	0.1−1.1	0.7−6	189.3	0.00325	0.2526	6.41	33.6
8	50	0.1−1.1	0.8−6	747.9	0.00131	0.2947	9.23	48.9
16	45	0.1−1.1	0.8−6	2702	0.000579	0.3898	14.3	40.8

[a]The number of points, density and temperature range of optimization and the Average Absolute and Maximal Deviation (AAD% and MxD%, respectively) are also included.

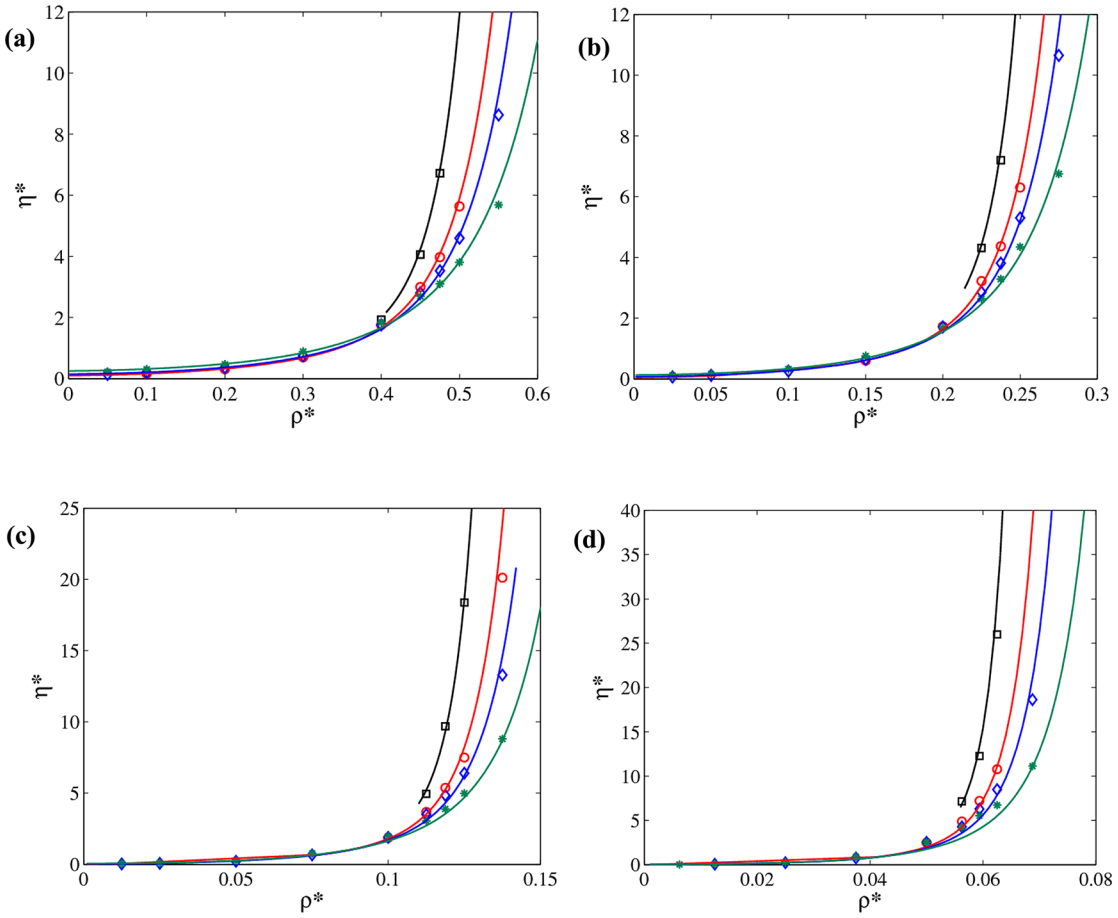

Figure 2. Reduced viscosity of Lennard-Jones chains. Viscosity−density diagram at four isotherms T* = 1.0 (black square), 2.0 (red circle), 3.0 (blue diamond), and 6.0 (green asterisk) of the (a) Lennard-Jones dimer (m = 2), (b) Lennard-Jones tetramer (m = 4), (c) Lennard-Jones octamer (m = 8), and (d) Lennard-Jones hexadecamer (m = 16). In all panels, symbols represent the experimental data,[16] while the curves correspond to the soft-SAFT + FVT modeling.

Later on, another modification based on the inclusion of the chain length was proposed by the same authors,[64] in order to be consistent with the results that they obtained using a rigid model instead of a fully flexible model. In our modified Chapman-Enskog version, the correction introduced by Chung is not converging to the zero-density value and this causes an increase of the error. Possibly, this may also be related to an incorrect description of the second virial viscosity coefficient B_η (do not confuse with the free-overlap parameter B). The second virial viscosity coefficient is defined by

$$\eta = \eta_0(1 + B_\eta\rho + ...) \quad (22)$$

It has been shown in the bibliography that there is a linear initial low-density viscosity dependence (apart from the temperature dependence) responsible for the behavior of the second viscosity virial coefficient.[67] This coefficient becomes negative at low reduced temperatures (T* < 1) and rapidly decreases with decreasing temperature, as observed for some substances like propane, benzene, methanol, and water.[68−70] In the formulation of FVT used in this work, the dilute gas term of Chung et al. only considers the zero-density limit, whereas the weak linear density dependence term is omitted. In this case, the free-volume dense term can be seen as the residual contribution that considers the effect of increasing density, but there is not a specific term for considering the linear initial density dependence.

Based on the empirical equation proposed by Vogel et al.[69] and followed in the work of Quiñones-Cisneros and Deiters,[10] eq 22 can be cut after the second term and rearranged to express the viscosity coefficient as

dx.doi.org/10.1021/jp401307t | J. Phys. Chem. B 2013, 117, 8159−8171

$$B_\eta = \frac{\left(\frac{d\eta}{d\rho}\right)_{\rho=0}}{\eta_0} \tag{23}$$

The derivation of the free-volume term at the zero-density limit provides the following result:

$$B_\eta = \frac{1}{\eta_0} 10^{-5} L_v \sqrt{\frac{0.1RTM_w}{3}} \exp(B) \tag{24}$$

Hence, the second virial viscosity coefficient will depend on the temperature and the B and L_v parameters. As in this work it is assumed these parameters are temperature independent and always positive, the calculation of the virial coefficient will never become negative, failing to reproduce this feature at low temperatures. Although this issue is important, it has been noted (as will be seen in next section), that very accurate prediction of the low-density (vapor density) of real compounds, such as *n*-alkanes, can be obtained with the current methodology in the range of temperature and pressure evaluated in this contribution. The revision of the theory in order to include a specific term for an accurate representation of the second virial viscosity coefficient does not fit into the scope of the present work.

An analysis of the three viscosity parameters reveals interesting trends, shown in Figure 3. The activation energy parameter α^* increases with the chain length following a parabolic trend. However, the ratio between α^*/m and m is a nearly perfect straight line (see Figure 3a). Considering the fact that the nonreduced value of α (with units) will be multiplied by the molecular weight in experimental compounds (the equivalent to the number of monomers in the simulations, see eq 19), it is expected to find a linear trend when studying a family of real compounds like *n*-alkanes. The increase on the activation energy with the chain length is expected, as it is believed that the molecules will need more energy to diffuse in other molecules when the molecular size increases.

The free-volume-overlap parameter B follows a contrary trend and it diminishes with the chain length till reaching a plateau at high values of m (see Figure 3b). As B is related to the empty space between molecules to overlap, the longer the molecules are, the fewer free space available there is.

Finally, the length parameter L_v increases almost linearly with the chain length (see Figure 3c). This parameter is a bit more difficult to interpret, as it is related to the structure of the molecule and the characteristic relaxation time. The three parameters can be correlated with the number of monomers using the following equations:

$$a^*/m = 11.426m + 1.524 \tag{25}$$

$$B^* = 1.644 \times 10^{-2} m^{(-1.20)} \tag{26}$$

$$L_v{}^* = 0.0124m + 0.1981 \tag{27}$$

In order to check the accuracy of these correlations, only information for LJ spheres till octamers has been included to build previous equations. From them, the values for $m = 16$ are predicted. As it can be observed in Figure 2d, the soft-SAFT viscosity curves are in good agreement with the simulation points, allowing the exploration of longer chain fluids for which there is no information about their viscosity.

3.2. Comparison to Experimental Systems. After checking the accuracy of the theory by comparing with molecular simulations, we applied it to experimental data, choosing the *n*-alkanes family, as a model family, for this purpose.

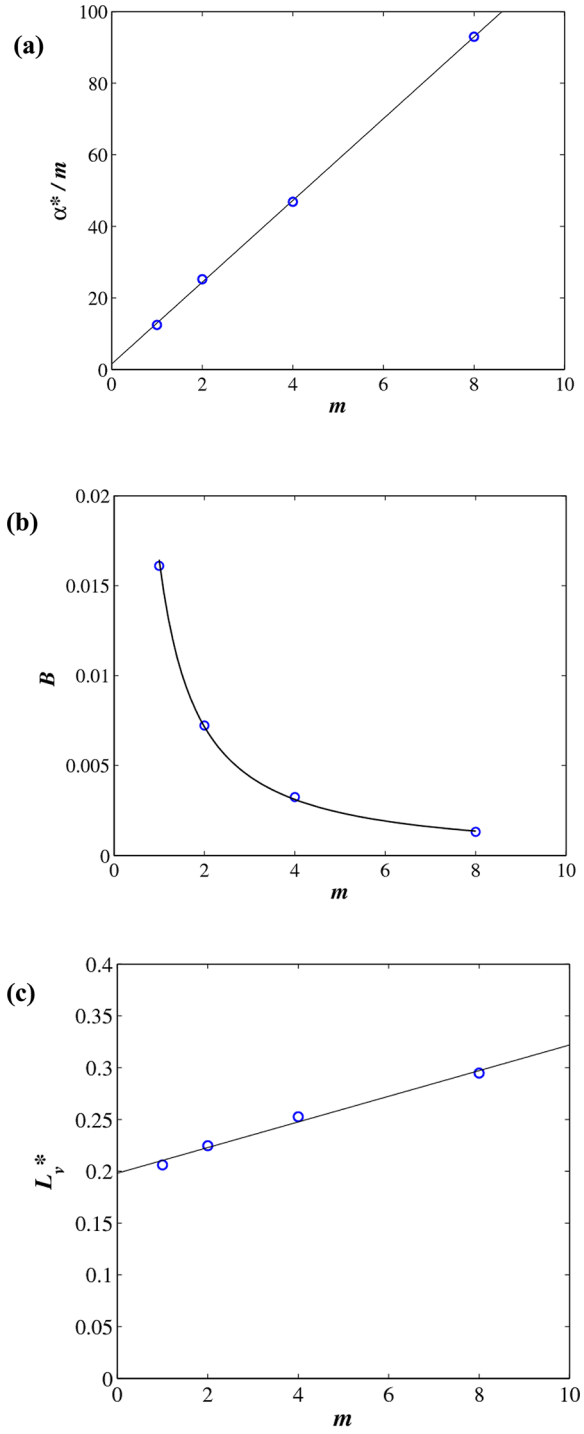

Figure 3. Correlations of (a) α^*, (b) B^*, and (c) L_v^* with the number of monomers (eqs 25−27, continuous lines).

3.2.1. Viscosity of n-Alkanes. The *n*-alkanes family is probably the most well studied family of organic compounds. As mentioned before, the thermodynamic properties of these compounds have been widely modeled by many authors. In terms of transport properties and, in particular, of viscosity, the *n*-alkanes have been calculated in some contributions using FVT,[6,25,29] the friction theory,[8,10,25,26,29,71,72] scaling viscosity-entropy methods,[14,15] and a LJ equation obtained from molecular dynamics simulations.[16,18,19] Here, we intend to

dx.doi.org/10.1021/jp401307t | J. Phys. Chem. B 2013, 117, 8159−8171

Table 2. Optimized Characteristic Parameters of FVT for the *n*-Alkanes Family[a]

compound	formula	N_{points}	P range (MPa)	T range (K)	α (J m^3/mol kg)	B	L_v (Å)	AAD (%)	MxD (%)
methane	CH_4	155	0.1−60	95−450	34.60	0.009573	0.5214	1.71	7.15
ethane	C_2H_6	170	0.1−60	120−450	41.43	0.009505	0.8920	2.57	7.92
propane	C_3H_8	170	0.1−60	150−450	53.90	0.008980	0.8919	2.55	6.34
butane	C_4H_{10}	140	0.1−60	200−450	64.28	0.008599	0.8824	2.65	7.86
pentane	C_5H_{12}	160	0.1−60	220−450	74.39	0.008140	0.8724	1.85	6.09
hexane	C_6H_{14}	125	0.1−60	220−450	84.21	0.007796	0.8628	1.84	3.18
heptane	C_7H_{16}	120	0.1−60	250−450	94.80	0.007149	0.8520	0.44	2.62
octane	C_8H_{18}	100	0.1−60	250−500	106.7	0.006743	0.8432	0.83	2.70
decane	$C_{10}H_{22}$	100	0.1−60	270−600	132.4	0.005968	0.8270	2.39	7.37
dodecane	$C_{12}H_{26}$	100	0.1−60	300−600	154.4	0.005529	0.8067	2.38	9.21
hexadecane	$C_{16}H_{34}$	23	0.1−49	293−532	208.0	0.004440	0.7746	2.65	8.61
eicosane	$C_{20}H_{42}$	8	0.1−1.4	313−534	261.4	0.003706	0.7400	3.61	8.39

[a]The number of points, pressure and temperature range of optimization and the AAD% and MxD%, respectively, are also included.

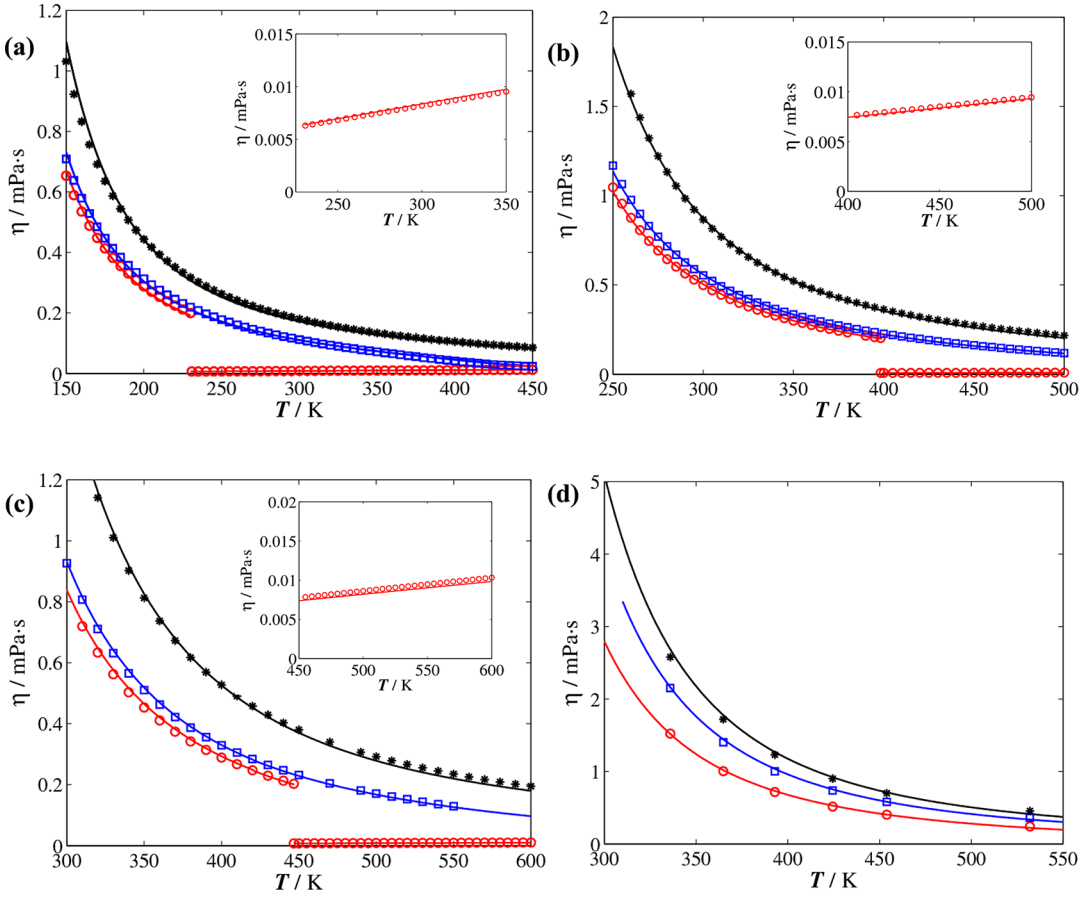

Figure 4. Viscosity as a function of temperature at a constant pressure of 0.1 (red cricle), 10 (blue square), and 60 MPa (black asterisk) of (a) propane, (b) *n*-octane, and (c) *n*-decane. (d) Viscosity as a function of temperature at a constant pressure of 0.098 (red circle), 29.4 (blue square), and 49 MPa (black asterisk) of *n*-hexadecane. The insets in panels a−c are enlargements of the vapor viscosity part of the graphic. Symbols represent the experimental data,[73,74] and the curves correspond to the soft-SAFT + FVT modeling.

describe the viscosity using a transferable approach, in the same way we have done in previous work for the optimization of the soft-SAFT molecular parameters, necessary for the description of the vapor−liquid equilibria.[31,35]

n-Alkanes are nonassociating compounds described as homonuclear chainlike molecules, modeled as m Lennard-Jones segments of equal diameter, σ_{ii}, and the same dispersive energy, ε_{ii}, bonded to form the chain. These molecular parameters are taken from previous work.[31] Two crossover parameters are also included for a correct density description in the critical region. They are also taken from the same source.

The three parameters of FVT were optimized using correlated experimental viscosity data from NIST,[73] excepting for *n*-hexadecane[71,74] and *n*-eicosane,[71,75] whose data were not available in the NIST database. The viscosity parameters from methane to *n*-dodecane have been found by fitting these parameters to the liquid viscosity of these compounds at four different isobars, selected randomly, to cover a wide range of thermodynamic conditions. In particular, isobars at 0.1 MPa, 1,

dx.doi.org/10.1021/jp401307t | J. Phys. Chem. B 2013, 117, 8159−8171

10, and 60 MPa have been chosen. For *n*-hexadecane and *n*-eicosane, the viscosity parameters were fitted to the available data (up to 49.4 MPa for *n*-hexadecane and up to 1.38 MPa for *n*-eicosane). The range of temperature changes for each compound and isobar, but it was chosen to cover a wide range of conditions up to at least 450 K. The final set of viscosity parameters, the number of experimental/correlated points used, the temperature and pressure ranges, and the AAD % and MxD% for each compound are indicated in Table 2.

In all cases, the deviation with the experimental data is low (see Table 2), with the highest deviation for the *n*-eicosane molecule, possibly due to the use of different experimental sources. In order to better appreciate those results, the viscosity of propane, *n*-octane and *n*-decane at 0.1, 10, and 60 MPa have been plotted in Figure 4a–c, respectively (the isobar at 1 MPa was relatively close to the one at 0.1 MPa and it is not shown in the figure to better appreciate the curves). Figure 4d includes the viscosity of *n*-hexadecane at 0.098, 29.4, and 49.8 MPa. The description of the viscosity with the theory is in very good agreement with the experimental data, with the major deviations at the highest isobar (60 MPa) and low temperatures. In Figure 4a–c, the viscosity of the vapor phase at the lowest isobar has also been calculated and plotted (see the inset of each figure for a zoom of this region). As it can be observed, the modified diluted term of Chung et al.[50] provides very good agreement with the experimental data (the dense term contribution is very small as the density approaches zero values) in the regions explored, contrarily to what was observed for the zero-density viscosity of long LJ chains. However, in this case, some variables such as the acentric factor or the critical properties are very well-known and this can explain the better performance for real fluids. Therefore, although having in mind the limitation of the current approach in predicting the second virial viscosity coefficient at low temperatures, FVT allows an accurate calculation of the viscosity in both the vapor and liquid phases using the same set of parameters for *n*-alkanes.

An additional remark is the possibility of having an accurate enhanced flattening of the viscosity as a function of pressure at the critical isotherm. In Figure 5a, the viscosity–pressure diagram of ethane, *n*-propane, and *n*-butane at their respective near-critical isotherms is shown. The comparison with the experimental data from NIST[73] shows very good agreement with the predicted viscosities (they are predictions because these data were not included in the fitting). The typical enhanced flattening of the critical isotherm comes from the pressure–density critical anomaly, which is a natural consequence of the competitive long-range interactions, affecting the pressure–density diagram. As the renormalization-group treatment applied corrects the typical overprediction of the critical point in SAFT-type equations and provides the right pressure–density diagram shape in the critical region, the viscosity-pressure diagram at the critical isotherm can be then properly addressed, as seen in Figure 5a. In fact, this flatness can be achieved without the need of a specific renormalization-treatment, but with an EoS intrinsically slow-convergent at the critical point. A second, and more particular anomaly related to viscosity, is a near-critical smooth viscosity enhancement that is observed in the viscosity-density diagram. According to Quiñones-Cisneros and Deiters,[10] this feature follows from an increased competitiveness between the attractive and repulsive contributions to the total pressure of the system. In Figure 5b, we show the viscosity–density diagram for propane at the same near-critical isotherm. Contrarily to the viscosity–pressure

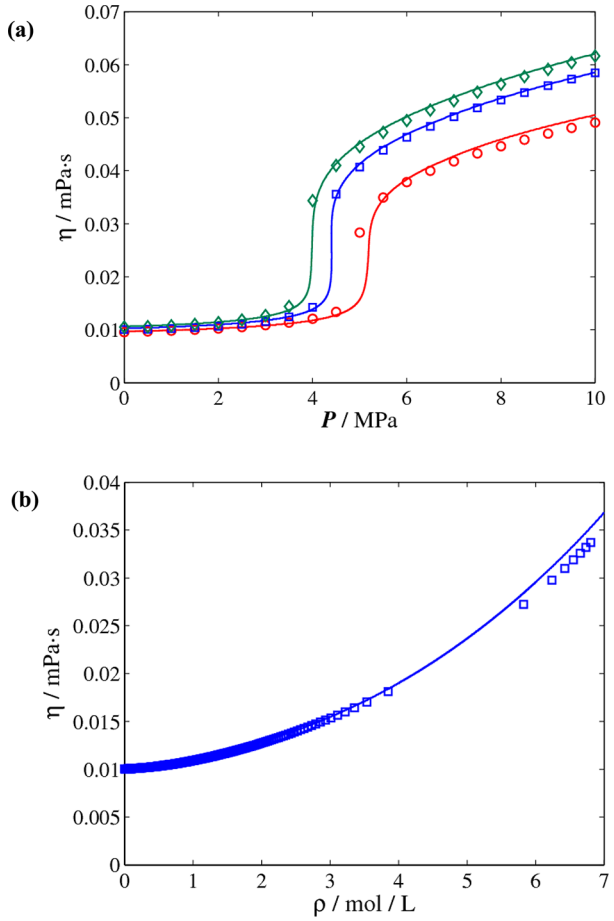

Figure 5. Viscosity at the near-critical isotherm: (a) viscosity–pressure diagram of ethane (T = 306 K; red circle), *n*-propane (T = 370 K; blue square), and *n*-butane (T = 426 K; green diamond). (b) Viscosity-density diagram of *n*-propane (T = 370 K) (blue square). Symbols represent the experimental data,[73] and the curves correspond to the soft-SAFT + FVT modeling.

diagram, no viscosity enhancement is observed in the critical region. This is probably due to the formulation of the FVT, which is strongly dependent on density but weakly dependent on pressure.

However, the previous anomalies should not be confused with the critical singularity of the viscosity observed in the vicinity of the critical point. Experimental measurements have confirmed the existence of a weak "critical singularity" of the viscosity, restricted to a very small region around the critical point. The critical viscosity enhancement is a multiplicative enhancement, i.e., the singular viscosity $\Delta\eta_c$ is proportional to the normal viscosity η.[76] The theory of dynamical critical phenomena predicts that the viscosity ratio $\Delta\eta_c/\eta$ will diverge as the correlation length ξ^z, where z is a critical viscosity exponent

$$\frac{\Delta\eta_c}{\eta} = (Q\xi)^z \tag{28}$$

Q is an amplitude that weakly depends on density and temperature and it is different for each system. This singular behavior should be addressed with a specific crossover treatment, such as the models developed by Sengers and co-workers.[77,78] The renormalization-group approach of White used in this work for the critical region has been only developed

dx.doi.org/10.1021/jp401307t | J. Phys. Chem. B 2013, 117, 8159–8171

for the estimation of the long-range fluctuations of the density, and an additional analogous treatment would be required to consider these viscosity fluctuations. However, as shown in several works,[79,80] the critical enhancement is restricted to a very small region around the critical point with a ratio $\Delta\eta_c/\eta$ smaller than 1%. Hence, due to the complexity of the additional treatment and the negligible consequences for the region investigated in this work, we have omitted this contribution and left it for further developments in the future.

As for the LJ chains, it has been possible to identify for the *n*-alkanes several trends of the viscosity parameters related to the molecular weight. As observed in the work of Tan et al.,[25] and later confirmed by Burgess et al.,[29] the fitting of several parameters leads to multivariable optimization and a non-uniqueness issue; multiple sets of parameters can fit the viscosity equally well for each substance. Following a similar approach, and based on the same spirit done for the soft-SAFT molecular parameters, we have tried to identify physical trends behind the viscosity parameters to discriminate among different sets of solutions. First of all, we have observed an increase of the barrier energy parameter α value with the molecular weight of the *n*-alkane, which allows the establishment of a linear relationship. A similar behavior was observed when this value was fitted to LJ chains, and it seems that the energy barrier is proportionally affected by the molecular weight of the compound (at least for linear molecules). The result obtained here is also in agreement with the parameter values obtained in the work of Tan et al. and Burgess et al. for PC-SAFT,[25,29] and corroborates the trend found in the original work of Allal et al.,[6] although in the latter case the parameter fitted was E_0, proportional to α as $E_0=\alpha\rho M_w$ (second term of eq 10). For the case of the free-volume overlap parameter B, it decreases with the molecular weight, in agreement with that observed for LJ chains, although in this case an exponential function with the molecular weight describes better its behavior. Here, the comparison with the work of Tan et al. is not worthy because there is not a clear tendency for B in their work. On the other hand, a very similar behavior to our results was obtained in the work of Burgess et al., also modeling the B trend with an exponential function. We believe that a decrease of the free-volume of overlap is expectable when the size of the molecules is increased. Finally, we have also observed that the length parameter L_v tends to decrease almost linearly with the molecular weight (with the exception of methane, which is completely out of the trend). In this case, we obtain the opposite behavior to that observed with LJ chains, where there was a very slight increase. This does not mean that the results are incoherent, since the internal degrees of freedom of *n*-alkanes are not the same than those of flexible LJ chains. In the work of Tan et al., there is not a clear trend for L_v, whereas in the work of Burgess et al., the same behavior observed in our work was found, and a linear correlation with the molecular weight was proposed. All of these trends are plotted in Figure 6. It is important to note that the establishment of these relations is done in order to make the methodology more predictive, allowing the prediction of the viscosity parameters of other compounds of the same family not included in the fitting. For that purpose, the following equations are proposed:

$$\alpha = 0.857M_w + 13.06 \tag{29}$$

$$B = 1.062\ e^{(-3.813\times10^{-3}M_w)} \tag{30}$$

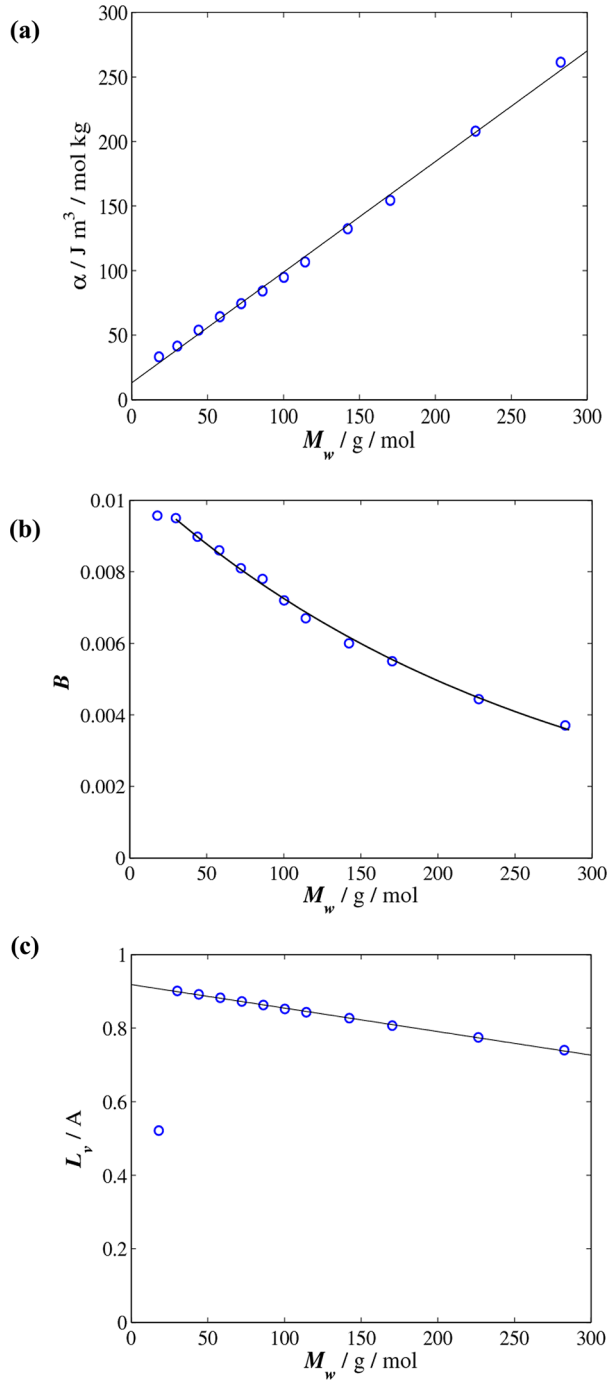

Figure 6. Correlations of (a) α, (b) B, and (c) L_v with M_w for the *n*-alkane molecules (eqs 29−31, continuous lines).

$$L_v = -6.39\times10^{-4}M_w + 0.918 \tag{31}$$

In order to test the accuracy of these correlations, we have checked the viscosity of three compounds not included in the fitting. The viscosity as a function of temperature at atmospheric pressure for *n*-octadecane ($C_{18}H_{38}$), *n*-docosane ($C_{22}H_{46}$), and *n*-tetracosane ($C_{24}H_{50}$) has been plotted in Figure 7. The lines are the soft-SAFT predictions and the symbols correspond to some experimental data available for those compounds.[71,81,82] Using eqs 29−31, we have calculated α, B, and L_v for these compounds. In general, there is good agreement between the experiments and the predictions,

dx.doi.org/10.1021/jp401307t | J. Phys. Chem. B 2013, 117, 8159−8171

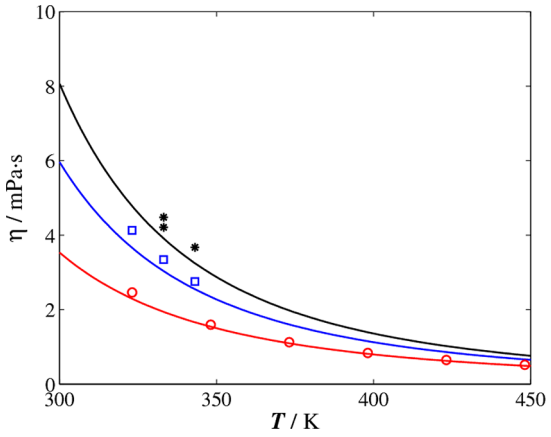

Figure 7. Predictions of the viscosity as a function of temperature at atmospheric pressure for *n*-octadecane (red circle), *n*-docosane (blue square), and *n*-tetracosane (black asterisk). Symbols represent the experimental data,[71,81,82] and the curves correspond to the soft-SAFT + FVT predictions.

although some deviations are observed for the heavier two *n*-alkanes. For the case of *n*-octadecane (see the red line) note that, although not included in the fitting, the predicted values lie in the range where the parameters were fitted (as far as *n*-eicosane is included). Predictions for *n*-octadecane are in very good agreement (AAD of 3.19%) with the data of Caudwell et al.[81] in the whole range of temperatures evaluated. For the case of *n*-docosane and *n*-tetracosane, whose viscosity parameters are extrapolated outside the range of the fitting, the comparison with experimental data[71,82] reveals a slight underestimation of the viscosity (AAD of 9.18% and 10.0%, respectively). Considering that a very minor change in the parameters at low temperature has a high impact in the viscosity, this could be related to some small deviations in the correlations. Conversely, the fact that there are very few experimental data and a higher degree of uncertainty in the same data (and also on the evaluation of the critical properties necessary for the calculations of the dilute term) does not allow providing more information. In any case, and looking at the current results, a reasonable description of the viscosity is expected to be found for the whole *n*-alkanes family. The performance of these parameters for mixtures will be presented in a forthcoming publication.

4. CONCLUSIONS

FVT has been coupled with the accurate soft-SAFT EoS for the simultaneous calculation of thermodynamic and transport properties. The theory has been implemented following the original papers of Allal and co-workers. The pressure (or temperature) and the density are taken from the original soft-SAFT EoS. The new treatment includes three parameters fitted to viscosity data, and trends with the molecular weight have been identified for each of them, empowering the method with the ability to predict the viscosity for other members of the family not included in the fitting procedure.

First, the soft-SAFT + FVT has been tested using molecular simulation data for the same underlying molecular model. Good agreement has been found with the simulations available in the literature for LJ chains, although some deviations for the zero-density viscosity at long chain lengths have been observed. The three viscosity parameters can be correlated with the number of monomers, allowing the prediction of other LJ chains not included in the original correlations.

In a second step, the new equation has been applied the *n*-alkanes family. A wide variety of *n*-alkanes, from methane to *n*-eicosane, have been studied. A simple molecular model is used with the soft-SAFT EoS for the description of the thermodynamic properties of these alkanes before proceeding to the calculation of the transport properties. Once the density and pressure of each compound is well determined, the FVT approach has been used, reaching very good agreement with the experimental data for all cases (AAD ranging between 0.44% and 3.61%) in a wide range of temperature and pressure, including predictions along the critical isotherm. All viscosity parameters have been related to the molecular weight, and a correlation for each one of them has been given in order to predict the parameters of other compounds of the same family. The use of these correlations has allowed the description of the viscosity of *n*-octadecane, *n*-docosane, and *n*-tetracosane in quite good agreement with the experimental data available.

In summary, this work is a first step toward the combination of a sound molecular-based EoS such as soft-SAFT, together with FVT, for an accurate prediction of both thermodynamic and transport properties using relatively simple models. The extension of the approach to mixtures and its performance for experimental mixtures of industrial interest will be presented in a forthcoming publication.

■ ASSOCIATED CONTENT

Supporting Information

Soft-SAFT molecular parameters and the results for the density−temperature diagram versus LJ chains and *n*-alkanes. This material is available free of charge via the Internet at http://pubs.acs.org.

■ AUTHOR INFORMATION

Corresponding Author

*E-mail: fllovell@matgas.org.

Notes

The authors declare no competing financial interest.

■ ACKNOWLEDGMENTS

F.L. acknowledges a TALENT fellowship from the Generalitat de Catalunya. This work was partially financed by the Spanish Government under Projects CTQ2008-05370/PPQ and CENIT SOST-CO2, CEN-2008-1027. Additional support from Carburos Metálicos, Air Products Group, and the Catalan Government was also provided (2009SGR-666).

■ REFERENCES

(1) Monnery, W. D.; Svrcek, W. Y.; Mehrotra, A. Viscosity: A Critical Review of Practical Predictive and Correlative Methods. *Can. J. Chem. Eng.* **1995**, *73*, 3−40.

(2) Reid, R. C.; Prausnitz, J. M.; Poling, B. E. *The Properties of Gases and Liquids*; McGraw-Hill: New York, 1987.

(3) Viswanath, D. S.; Ghosh, T. K.; Prasad, D. H. L.; Dutt, N. K; Rani, K. Y. *Viscosity of Liquids. Theory, Estimation, Experiment, and Data*; Springer: Dordrecht, The Netherlands, 2006.

(4) Dymond, J. H.; Awan, M. A. Correlation of High-Pressure Diffusion and Viscosity Coefficients for *n*-Alkanes. *Int. J. Thermophys.* **1989**, *10*, 941−951.

(5) Assael, M. J.; Dymond, J. H.; Papadaki, M.; Patterson, P. M. Correlation and Prediction of Dense Fluid Transport Coefficients: II. Simple Molecular Fluids. *Fluid Phase Equilib.* **1992**, *75*, 245−255.

(6) Allal, A.; Moha-Ouchane, M.; Boned, C. A New Free Volume Model for Dynamic Viscosity and Density of Dense Fluids Versus Pressure and Temperature. *Phys. Chem. Liq.* **2001**, *39*, 1−30.
(7) Allal, A.; Boned, C.; Baylaucq, A. Free-Volume Viscosity Model for Fluids in the Dense and Gaseous States. *Phys. Rev. E* **2001**, *64*, 011203.
(8) Quiñones-Cisneros, S. E.; Zéberg-Mikkelsen, C. K.; Stenby, E. H. The Friction Theory (f-theory) for Viscosity Modeling. *Fluid Phase Equilib.* **2000**, *169*, 249−276.
(9) Quiñones-Cisneros, S. E.; Zéberg-Mikkelsen, C. K.; Stenby, E. H. One Parameter Friction Theory Models for Viscosity. *Fluid Phase Equilib.* **2001**, *178*, 1−16.
(10) Quiñones-Cisneros, S. E.; Deiters, U. K. Generalization of the Friction Theory for Viscosity Modeling. *J. Phys. Chem. B* **2006**, *110*, 12820−12834.
(11) de Wijn, A. S.; Vesovic, V.; Jackson, G.; Trusler, J. P. M. A Kinetic Theory Description of the Viscosity of Dense Fluids Consisting of Chain Molecules. *J. Chem. Phys.* **2008**, *128*, 204901.
(12) Srivastava, R.; Dwivedee, D. K.; Khanna, K. N. Scaling Laws for Transport Coefficients of a Hard Sphere Fluid. *J. Mol. Liq.* **2008**, *139*, 29−34.
(13) Goel, T.; Patra, C. N.; Mukherjee, T.; Chakravarty, C. Excess Entropy Scaling of Transport Properties of Lennard-Jones Chains. *J. Chem. Phys.* **2008**, *129*, 164904.
(14) Galliero, G.; Boned, C.; Fernández, J. Scaling of the Viscosity of the Lennard-Jones Chain Fluid Model, Argon and Some Normal Alkanes. *J. Chem. Phys.* **2011**, *134*, 064505.
(15) Novak, L. T. Fluid Viscosity-Residual Entropy correlation. *Int. J. Chem. React. Eng.* **2011**, *9*, A107.
(16) Galliero, G.; Boned, C.; Baylaucq, A. Molecular Dynamics Study of the Lennard−Jones Fluid Viscosity: Application to Real Fluids. *Ind. Eng. Chem. Res.* **2005**, *44*, 6963−6972.
(17) Galliero, G.; Boned, C. Shear Viscosity of the Lennard-Jones Chain Fluid in its Gaseous, Supercritical, and Liquid States. *Phys. Rev. E* **2009**, *79*, 021201.
(18) Zabaloy, M. S.; Machado, J. M. V.; Macedo, E. A. A Study of Lennard-Jones Equivalent Analytical Relationships for Modeling Viscosities. *Int. J. Thermophys.* **2001**, *22*, 829−858.
(19) Zabaloy, M. S.; Vasquez, V. R.; Macedo, E. A. Viscosity of Pure Supercritical Fluids. *J. Supercrit. Fluids.* **2005**, *36*, 106−117.
(20) Boned, C.; Allal, A.; Baylaucq, A.; Zéberg-Mikkelsen, C. K.; Bessières, D.; Quiñones-Cisneros, S. E. Simultaneous Free-Volume Modeling of the Self-Diffusion Coefficient and Dynamic Viscosity at High Pressure. *Phys. Rev. E* **2004**, *69*, 031203.
(21) Baylaucq, A.; Comuñas, M. J. P.; Boned, C.; Allal, A.; Fernández, J. High Pressure Viscosity and Density Modeling of Two Polyethers and Two Dialkyl Carbonates. *Fluid Phase Equilib.* **2002**, *199*, 249−263.
(22) Zéberg-Mikkelsen, C. K.; Baylaucq, A.; Barrouhou, M.; Boned, C. The Effect of Stereoisomerism on Dynamic Viscosity: A Study of cis-Decalin and trans-Decalin Versus Pressure and Temperature. *Phys. Chem. Chem. Phys.* **2003**, *5*, 1547−1551.
(23) Comuñas, M. J. P.; Baylaucq, A.; Plantier, F.; Boned, C.; Fernández, J. Influence of the Number of CH_2−CH_2−O Groups on the Viscosity of Polyethylene Glycol Dimethyl Ethers at High Pressure. *Fluid Phase Equilib.* **2004**, *222*−*223*, 331−338.
(24) Reghem, P.; Baylaucq, A.; Comuñas, M. J. P.; Fernández, J.; Boned, C. Influence of the Molecular Structure on the Viscosity of Some Alkoxyethanols. *Fluid Phase Equilib.* **2005**, *236*, 229−236.
(25) Tan, S. P.; Adidharma, H.; Towler, B. F.; Radosz, M. Friction Theory and Free-Volume Theory Coupled with Statistical Associating Fluid Theory for Estimating the Viscosity of Pure *n*-Alkanes. *Ind. Eng. Chem. Res.* **2005**, *44*, 8409−8418.
(26) Tan, S. P.; Adidharma, H.; Towler, B. F.; Radosz, M. Friction Theory Coupled with Statistical Associating Fluid Theory for Estimating the Viscosity of *n*-Alkane Mixtures. *Ind. Eng. Chem. Res.* **2006**, *45*, 2116−2122.
(27) Quiñones-Cisneros, S. E.; Zéberg-Mikkelsen, C. K.; Fernández, J.; García, J. General Friction Theory Viscosity Model for the PC-SAFT Equation of State. *AIChE J.* **2006**, *52*, 1600−1610.
(28) Polishuk, I. Modeling of Viscosities in Extended Pressure Range Using SAFT + Cubic EoS and Modified Yarranton-Satyro Correlation. *Ind. Eng. Chem. Res.* **2012**, *51*, 13527−13537.
(29) Burgess, W. A.; Tapriyal, D.; Gamwo, I. K.; Morreale, B. D.; McHugh, M. A.; Enick, R. M. Viscosity Models Based on the Free Volume and Frictional Theories for Systems at Pressures to 276 MPa and Temperatures to 533 K. *Ind. Eng. Chem. Res.* **2012**, *51*, 16721−16733.
(30) Blas, F. J.; Vega, L. F. Thermodynamic Behaviour of Homonuclear and Heteronuclear Lennard-Jones Chains with Association Sites from Simulation and Theory. *Mol. Phys.* **1997**, *92*, 135−150.
(31) Llovell, F.; Pàmies, J. C.; Vega, L. F. Thermodynamic Properties of Lennard-Jones Chain Molecules: Renormalization-Group Corrections to a Modified Statistical Associating Fluid Theory. *J. Chem. Phys.* **2004**, *121*, 10715−10724.
(32) Llovell, F.; Vega, L. F. Global Fluid Phase Equilibria and Critical Phenomena of Selected Mixtures Using the Crossover Soft-SAFT Equation. *J. Phys. Chem. B* **2006**, *110*, 1350−1362.
(33) Blas, F. J.; Vega, L. F. Prediction of Binary and Ternary Diagrams Using the Statistical Associating Fluid Theory (SAFT) Equation of State. *Ind. Eng. Chem. Res.* **1998**, *37*, 660−674.
(34) Blas, F. J.; Vega, L. F. Critical Behavior and Partial Miscibility Phenomena in Binary Mixtures of Hydrocarbons by the Statistical Associating Fluid Theory. *J. Chem. Phys.* **1998**, *109*, 7405−7413.
(35) Pàmies, J. C.; Vega, L. F. Vapor-Liquid Equilibria and Critical Behavior of Heavy n-Alkanes Using Transferable Parameters from the Soft-SAFT Equation of State. *Ind. Eng. Chem. Res.* **2001**, *40*, 2532−2543.
(36) Florusse, L. J.; Pàmies, J. C.; Vega, L. F.; Peters, C. J.; Meijer, H. Solubility of Hydrogen in Heavy n-alkanes: Experiments and SAFT Modeling. *AIChE J.* **2003**, *49*, 3260−3269.
(37) Llovell, F.; Florusse, L. J.; Peters, C. J.; Vega, L. F. Vapor-Liquid and Critical Behavior of Binary Systems of Hydrogen Chloride and *n*-Alkanes: Experimental Data and Soft-SAFT Modeling. *J. Phys. Chem. B* **2007**, *111*, 10180−10188.
(38) Vega, L. F.; Llovell, F.; Blas, F. J. Capturing the Solubility Minima of n-Alkanes in Water by Soft-SAFT. *J. Phys. Chem. B* **2009**, *113*, 7621−7630.
(39) Dias, A. M. A.; Pàmies, J. C.; Coutinho, J. A. P.; Marrucho, I. M.; Vega, L. F. SAFT Modeling of the Solubility of Gases in Perfluoroalkanes. *J. Phys. Chem. B* **2004**, *108*, 1450−1457.
(40) Dias, A. M. A.; Carrier, H.; Daridon, J. L.; Pàmies, J. C.; Vega, L. F.; Coutinho, J. A. P.; Marrucho, I. M. Vapor-Liquid Equilibrium of Carbon Dioxide-Perfluoroalkane Mixtures: Experimental Data and SAFT Modeling. *Ind. Eng. Chem. Res.* **2006**, *45*, 2341−2350.
(41) Dias, A. M. A; Llovell, F.; Coutinho, J. A. P.; Marrucho, I. M.; Vega, L. F. Thermodynamic Characterization of Pure Perfluoroalkanes, Including Interfacial and Second Order Derivative Properties, Using the Crossover Soft-SAFT EoS. *Fluid Phase Equilib.* **2009**, *286*, 134−143.
(42) Vilaseca, O.; Llovell, F.; Yustos, J.; Marcos, R. M.; Vega, L. F. Phase Equilibria, Surface Tensions and Heat Capacities of Hydrofluorocarbons and Their Mixtures Including the Critical Region. *J. Supercrit. Fluids* **2010**, *55*, 755−768.
(43) Andreu, J. S.; Vega, L. F. Capturing the Solubility Behavior of CO_2 in Ionic Liquids by a Simple Model. *J. Phys. Chem. C* **2007**, *111*, 16028−16034.
(44) Llovell, F.; Valente, E.; Vilaseca, O.; Vega, L. F. Modeling Complex Associating Mixtures with $[C_n\text{-mim}][Tf_2N]$ Ionic Liquids: Predictions from the Soft-SAFT Equation. *J. Phys. Chem. B* **2011**, *115*, 4387−4398.
(45) Oliveira, M. B.; Llovell, F.; Coutinho, J. A. P.; Vega, L. F. Modeling the $[NTf_2]$ Pyridinium Ionic Liquids Family and Their Mixtures with the Soft Statistical Associating Fluid Theory Equation of State. *J. Phys. Chem. B* **2012**, *116*, 9089−9100.
(46) Llovell, F.; Vilaseca, O.; Vega, L. F. Thermodynamic Modeling of Imidazolium-Based Ionic Liquids with the $[PF_6]^-$ Anion for Separation Purposes. *Sep. Sci. Technol.* **2012**, *47*, 399−410.

(47) Doolittle, A. K. Studies in Newtonian Flow. II. The Dependence of the Viscosity of Liquids on Free Space. *J. Appl. Phys.* **1951**, *22*, 1471−1475.
(48) Cohen, M. H.; Turnbull, D. Molecular Transport in Liquids and Gases. *J. Chem. Phys.* **1959**, *31*, 1164−1169.
(49) Reed, T. M.; Gubbins, K. E. *Applied Statistical Mechanics*; Mc Graw-Hill: New York, 1973.
(50) Chung, T. H.; Ajlan, M.; Lee, L. L.; Starling, K. E. Generalized Multiparameter Correlation for Nonpolar and Polar Fluid Transport Properties. *Ind. Eng. Chem. Res.* **1988**, *27*, 671−679.
(51) Neufeld, P. D.; Janzen, A. R.; Aziz, R. A. Empirical Equations to Calculate 16 of the Transport Collision Integrals $\Omega(l,s)^*$ for the Lennard-Jones (12-6) Potential. *J. Chem. Phys.* **1972**, *57*, 1100−1102.
(52) Hogenboom, D. L.; Webb, W.; Dixon, J. A. Viscosity of Several Liquid Hydrocarbons as a Function of Temperature, Pressure and Free Volume. *J. Chem. Phys.* **1967**, *46*, 2586−2598.
(53) Chapman, W. G.; Gubbins, K. E.; Jackson, G.; Radosz, M. SAFT Equation of State Solution Model for Associating Fluids. *Fluid Phase Equilib.* **1989**, *52*, 31−38.
(54) Chapman, W. G.; Gubbins, K. E.; Jackson, G.; Radosz, M. New Reference Equation of State for Associating Liquids. *Ind. Eng. Chem. Res.* **1990**, *29*, 1709−1721.
(55) Wertheim, M. S. Fluids with Highly Directional Attractive Forces. 1. Statistical Thermodynamics. *J. Stat. Phys.* **1984**, *35*, 19−34.
(56) Wertheim, M. S. Fluids with Highly Directional Attractive Forces. 2. Thermodynamic-Perturbation Theory and Integral-Equations. *J. Stat. Phys.* **1984**, *35*, 35−47.
(57) Wertheim, M. S. Fluids with Highly Directional Attractive Forces. 3. Multiple Attraction Sites. *J. Stat. Phys.* **1986**, *42*, 459−476.
(58) Wertheim, M. S. Fluids with Highly Directional Attractive Forces. 4. Equilibrium Polymerization. *J. Stat. Phys.* **1986**, *42*, 477−492.
(59) Johnson, J. K.; Zollweg, J. A.; Gubbins, K. E. The Lennard-Jones Equation of State Revisited. *Mol. Phys.* **1993**, *78*, 591−618.
(60) Johnson, J. K.; Müller, E. A.; Gubbins, K. E. Equation of State for Lennard-Jones Chains. *J. Phys. Chem.* **1994**, *98*, 6413−6419.
(61) White, J. A. Contribution of Fluctuations to Thermal Properties of Fluids with Attractive Forces of Limited Range: Theory Compared with $P\rho t$ And C_v Data for Argon. *Fluid Phase Equilib.* **1992**, *75*, 53−64.
(62) Salvino, L. W.; White, J. A. Calculation of Density Fluctuation Contributions to Thermodynamic Properties of Simple Fluids. *J. Chem. Phys.* **1992**, *96*, 4559−4568.
(63) White, J. A.; Zhang, S. Renormalization Group Theory for Fluids. *J. Chem. Phys.* **1993**, *99*, 2012−2019.
(64) Santacreu, S. D.; Galliero, G.; Odunlami, M.; Boned, C. Low Density Shear Viscosity of Lennard-Jones Chains of Variable Rigidities. *J. Chem. Phys.* **2012**, *137*, 204306.
(65) Galliero, G. Surface Tension of Short Flexible Lennard-Jones Chains: Corresponding States Behavior. *J. Chem. Phys.* **2010**, *133*, 074705.
(66) Blas, F. J.; Mac Dowell, L. G.; de Miguel, E.; Jackson, G. Vapor-Liquid Interfacial Properties of Fully Flexible Lennard-Jones Chains. *J. Chem. Phys.* **2008**, *129*, 144703.
(67) Rainwater, J. C.; Friend, D. G. Second Viscosity and Thermal-Conductivity Virial Coefficients of Gases: Extension to Low Reduced Temperature. *Phys. Rev. A* **1987**, *36*, 4062−4066.
(68) Vogel, E.; Bich, E.; Nimz, R. The Initial Density Dependence of the Viscosity of Organic Vapours: Benzene and Methanol. *Physica* **1986**, *139A*, 188−207.
(69) Vogel, E.; Küchenmeister, C.; Bich, E.; Laesecke, A. Reference Correlation of the Viscosity of Propane. *J. Phys. Chem. Ref. Data* **1998**, *27*, 947−970.
(70) Teske, V.; Vogel, E.; Bich, E. Viscosity Measurements on Water Vapor and Their Evaluation. *J. Chem. Eng. Data* **2005**, *50*, 2082−2087.
(71) Queimada, A. J.; Marrucho, I. M.; Coutinho, J. A. P; Stenby, E. H. Viscosity and Liquid Density of Asymmetric Hydrocarbon Mixtures. *Int. J. Thermophys.* **2003**, *26*, 1221−1239.
(72) Queimada, A. J.; Marrucho, I. M.; Coutinho, J. A. P; Stenby, E. H. Viscosity and Liquid Density of Asymmetric n-Alkane Mixtures: Measurement and Modeling. *Int. J. Thermophys.* **2005**, *26*, 47−61.
(73) NIST Chemistry Webbook; http://webbook.nist.gov/chemistry.
(74) Keramidi, A. S. Viskosität von Alkanen. *Izv. Vyssh. Uchebn. Zaved. Neft Gaz* **1972**, *1*, 61−66.
(75) Rodden, J. B.; Erkey, C.; Akgerman, A. High-Temperature Diffusion, Viscosity, and Density Measurements in *n*-Eicosane. *J. Chem. Eng. Data* **1988**, *33*, 344−347.
(76) Watson, J. T. R.; Basu, R. S.; Sengers, J. V. An Improved Representative Equation for the Dynamic Viscosity of Water Substance. *J. Phys. Chem. Ref. Data* **1980**, *9*, 1255−1290.
(77) Olchowy, G. A.; Sengers, J. V. Crossover from Singular to Regular Behavior of the Transport Properties of Fluids in the Critical Region. *Phys. Rev. Lett.* **1988**, *61*, 15−18.
(78) Luettmer-Strathmann, J.; Olchowy, G. A.; Sengers, J. V. Nonasymptotic Critical Behavior of the Transport Properties of Fluids. *J. Chem. Phys.* **1995**, *103*, 7482−7501.
(79) Vesovic, V.; Wakeham, W. A.; Olchowy, G. A.; Sengers, J. V.; Watson, J. T. R.; Millat, J. The Transport Properties of Carbon Dioxide. *J. Phys. Chem. Ref. Data* **1990**, *19*, 763−808.
(80) Hendl, S.; Millat, J.; Vogel, E.; Vesovic, V.; Wakeham, W. A.; Luettmer-Strathmann, J.; Sengers, J. V.; Assael, M. J. The Transport Properties of Ethane. I. Viscosity. *Int. J. Thermophys.* **1994**, *15*, 1−31.
(81) Caudwell, D. R.; Trusler, J. P. M.; Vesovic, V.; Wakeham, W. A. The Viscosity and Density of n-Dodecane and n-Octadecane at Pressures Up to 200 MPa and Temperatures Up to 473 K. *Int. J. Thermophys.* **2004**, *25*, 1339−1352.
(82) Design Institute for Physical Property Data; *DIPPR Database*; AIChE: New York, 1998.